Journal of Radioanalytical and Nuclear Chemistry (2023) 332:4101–4112
https://doi.org/10.1007/s10967-023-09102-0

Employment of Co(II)–Fe(III) layered double hydroxide as magnetic adsorbent for rapid recovery of molybdenum-99

Mohamed A. Ghamry[1] · Mohamed A. Attia[1] · Moustafa A. Hamoud[1] · Mamdoh R. Mahmoud[1]

Received: 8 May 2023 / Accepted: 5 August 2023 / Published online: 26 August 2023

Abstract

Co(II)–Fe(III) Layered double hydroxide (LDH) was prepared by co-precipitation methods for recovery of ^{99}Mo(VI) from aqueous solutions. The data showed that ^{99}Mo(VI) anions are efficiently adsorbed (R% > 98), in the pH range 2.5–11. The kinetic data showed that about 82% of ^{99}Mo(VI) are adsorbed onto the synthesized LDH in the first ten minutes, while the equilibrium is attained at 120 min. The thermodynamic parameters (ΔG°, ΔH° and ΔS°) are estimated in the temperature range 20–50 °C. The effect of different foreign anions, (Cl^-, SO_4^{2-}, $CO_3^{2-}$and NO^-_3) at various concentrations is evaluated. The synthesized adsorbent showed maximum adsorption capacity of 255.175 mg g^{-1} for ^{99}Mo(VI) at pH = 3.5, which is mostly higher than those reported in literature.

Keywords Layered double hydroxide (LDH) · Molybdenum · Recovery · Adsorption

Introduction

Molybdenum-99 (^{99}Mo (VI), $t_{1/2}$ = 66 h) is essentially produced as a fission product from U^{235} with high yield (6.13%) and high specific activity (> 104 Ci/g) [1–3]. Its decay to ^{99m}Tc ($t_{1/2}$ = 6 h), renders it one of the most important radionuclides. This daughter is the best radioactive isotopes applied in radiopharmaceuticals in nuclear medicine, accounting for closely 80–85% of all nuclear diagnostic tests and has not yet been substituted with any other radionuclides [4–6]. This is because of its relevant nuclear properties, such as its relatively low -ray energy at peak 140.5 keV, short half-life (6.0 h), and low radiation exposure [2, 7]. From the economic point of view, it is important to recover of ^{99}Mo(VI) radionuclides from solutions. For industrial applications, molybdenum is used as a reactor vessel, alloying agent in steels cast iron and in special batteries [8].

Ion exchange, solvent extraction, co-precipitation, membrane separation and adsorption as the conventional methods applied for recovery of ^{99}Mo(VI) from aqueous solutions [9–15]. The last one is the most commonly used methods one due to its simplicity and excellent performance. Adsorption of ^{99}Mo(VI) onto different adsorbents was studied [3, 7, 8, 16–19]. Owing to its high affinity towards molybdenum as well as its high radiation, thermal and chemical stability, alumina (Al_2O_3) is efficiently applied in nuclear institutions for molybdenum recovery. However, alumina has a relatively low molybdenum adsorption capacity ranging from 2 to 20 mg g^{-1} [19]. Many attempts have been studied to improve the capacity of Al_2O_3 for adsorption of ^{99}Mo(VI). Denkova.et al. synthesized mesoporous aluminum oxides Al-TUD-1 and achieved maximum adsorption capacity for Mo 112 mg g^{-1} at pH range 2–5 [6] Chakravarty et al. synthesized nanocrystalline γ-Al_2O_3 which a maximum sorption capacity for Mo 200 ± 5 mg g^{-1} at pH = 3[16]. Saptiama et al. synthesized mesoporous alumina spheres using post-synthesis water–ethanol treatment and reaching Mo adsorption capacity of 56.2 mg g^{-1} at pH 3 [20].

One of the most important materials adsorbed is layer double hydroxides (LDH) which consist of two valance metal ions, usually in the 2+ and 3+ oxidation state balanced with hydroxide and another counter ion [21]. The general formula for LDH is principally composed of positively charged host layers and exchangeable interlayer anions, which can be represent by: $[M_{1-x}^{2+}M_x^{3+}(OH)_2(A^{n-})_{x/n}\cdot mH_2O]$, where M^{2+} represents a divalent metal cation such as Mg^{2+}, Ca^{2+}, Mn^{2+}, Cu^{2+}, Zn^{2+}, Ni^{2+} and M^{3+} is a trivalent metal cation, such as Al^{3+}, Mn^{3+}, Fe^{3+}, Cr^{3+}, and Co^{3+}. A^{n-} is an inorganic anion, such as Cl^-, NO_3^-, CO_3^{2-} and SO_4^{2-}

✉ Mohamed A. Attia
m_attia85@yahoo.com

[1] Nuclear Chemistry Dept., Hot Lab Center, Egyptian Atomic Energy Authority, P.O. 13759 Cairo, Egypt

or an organic anion, [22–24]. Organic and inorganic anions can be presented between hydroxide layer by ion exchange or precipitation.

LDHs are important in technology, such as medical science, separation technology, optics and catalysis [25] and also used in commercial products act as polymer stabilizers and anion exchange [26]. They have several advantages such as, anion exchange capacity, pH-sensitivity response excellent biocompatibility, biodegradability, easy surface modification and biomedical application such as cancer therapy ant anti-bacteria [27]. Recently many LDHs were prepared for adsorption of some anions such as iodine anions by prepared Mg/Fe and Co/Cr LDH nanostructured [28], arsenate using a novel LDHs consisted of (Cu/Mg/Fe/La-LDH) [29], nitrate anion from artificial nitrate solution using Zn/Al chloride LDH which was synthesis and physicochemical characterization [30], estimated different controls on molybdate, arsenate, and selenite anions uptake by hydrotalcite-like layered double hydroxides (HT-LDHs) [31], synthesize Zn–Fe (LDHs) by co-precipitation methods to obtain vanadate-LDH and molybdate–LDH nanohybrids [32], removal of molybdenum [33] and antimony [34] from aqueous solution by synthesized Zn–Al sulphate (LDHs) was studied.

Despite the many advantages of LDH, its use as a solid phase in separation processes of different anions faces some problems. The incomplete phase separation of the solid from the liquid is considered as one of these problems, where some of LDH particles are suspended in the solution. So, it is preferred to use a membrane in such separation processes. To overcome this problem, iron is incorporated as a trivalent cation in synthesis process of LDH to improve its mechanical properties and acquire it some magnetic properties that are benefits in separation process.

The present study aims to synthesis Co(II)–Fe(III) LDH and apply it as magnetic materials for recovery of ^{99}Mo(VI) radionuclides from aqueous solutions.

Experimental

Chemicals and materials

Ferric chloride hexahydrate ($FeCl_3 \cdot 6H_2O$) and cobalt chloride hexahydrate ($CoCl_2 \cdot 6H_2O$) used in this study were obtained from Merck. Stock solutions of ^{99}Mo(VI) 500 mg L^{-1}, was prepared by dissolving the suitable amount of sodium molybdate dihydrate ($Na_2MoO_4 \cdot 2H_2O$, ACS reagent, ≥ 99% sigma) in distilled water. The radioactive ^{99}Mo(IV) was supplied from Radioisotope Production Facility (RPF), Egyptian Atomic Energy Authority at Inshas, Cairo, Egypt and was used as a radiotracer for molybdenum during adsorption experiments.

Sodium chloride (NaCl), sodium carbonate (Na_2CO_3), sodium sulfate (Na_2SO_4) and sodium nitrate ($NaNO_3$) were supplied from Sigma Aldrich. These salts were used as source of Cl^-, CO_3^{2-}, SO_4^{2-}, NO_3^- anions, respectively to study the effect of foreign ions during adsorption and desorption experiments. Hydrochloric acid (HCl, Sigma Aldrich) and sodium hydroxide (NaOH, Chem-Lab) were used to adjust the pH of the working solution during adsorption experiments.

Synthesis of Co(II)–Fe(III) LDH

In this study, the co-precipitation method was used to synthesis the Co(II)–Fe(III) LDH material. Certain amounts of $CoCl_2 \cdot 6H_2O$ and $FeCl_3 \cdot 6H_2O$ were separately dissolved in 250 mL distilled water to obtain concentrations of 0.3 and 0.1 mol/L, respectively. These solutions were mixed together with stirring continuously. Then NaOH (1M) solution was added drop wise until the pH of ≈ 10.7 was reached and the suspension was aged for 4 h at room temperature. The resultant precipitates were left to settle for 48 h before being filtered. After that, the precipitate was then washed with distilled water until the pH of supernatant reached to 7, separated by filtration and finally dried at 70 °C till constant weight.

Characterization of prepared sample

The surface properties of Co(II)–Fe(III) LDH were ascribed by the standard adsorption of N_2 gas using a Quantachrome NOVA 1000e surface area analyzer (USA).The Fourier transform infrared (FTIR) spectrum of the synthesized Co(II)–Fe(III) LDH obtained by a Nicolet iS10-FTIR spectrometer (USA) using KBr pellets in the range of 4000–400 cm^{-1} at a resolution of 4 cm^{-1}. The phase structure was studied using an X-ray diffractometer (XRD) equipment of Brukur advanced D8 Kristalloflex model using Ni-filtered and CuK_α radiation source.

Adsorption studies of ^{99}Mo(VI) radioactive isotope

The batch technique was used to investigate the adsorption behavior of ^{99}Mo(VI) on Co(II)–Fe(III) LDH material in 25 mL glass bottles using a thermostated water bath shaker (model SW-20C/2 from Julobo laboratories GmbH (Germany) at 30 ± 1 °C (except effect of temperature experiment). The kinetic experiments for adsorption of ^{99}Mo(VI) onto the Co(II)–Fe(III) LDH material were studied using 50 mg L^{-1} as an initial concentration and time range of 1–165 min at pH values of 3.5 and 9.5.The effect pH of the solutions on the removal efficiency of ^{99}Mo(VI) by Co(II)–Fe(III) LDH was achieved at pH ranging from 3.2 to 12.77 at initial concentration of 50 mg L^{-1} at temperature = 30 ± 1 °C and contact

time = 2 h. The pH of the solutions was adjusted to the desired value by adding diluted HCl or NaOH solution using pH meter (model 59,003/digital, OAKTON (Portugal). The suspensions were equilibrated for 2 h at 30 ± 1 °C using a thermostated water bath shaker. The effect of foreign anions (Cl^-, NO_3^-, CO_3^{2-} and SO_4^{2-}) on adsorption process of the ^{99}Mo(VI) onto Co(II)–Fe(III) LDH was achieved by mixing 5 mL of ^{99}Mo(VI) at initial concentration of 50 mg L^{-1} with 0.04 g Co(II)–Fe(III) LDH material at pH 3.5 and contact time of 2 h and different foreign ion concentrations. To determine the suitable LDH mass necessary to achieve efficient adsorption for ^{99}Mo(VI), different masses in the range (0.005–0.1 g) were added to the 5 mL solution of ^{99}Mo(VI) at initial concentration 50 mg L^{-1} and pH 3.5. The suspensions were equilibrated for 2 h. The effect of temperature at different values (20, 40 and 50 °C) on the adsorption efficiency of ^{99}Mo(VI) at initial concentration 200 mg L^{-1} by Co(II)–Fe(III) LDH was studied at pH 3 and contact time of 2 h. Adsorption isotherm experiments were performed with initial ^{99}Mo(VI) concentrations ranging from 4 to 350 mg L^{-1}.

In order to study the Co(II)–Fe(III) LDHs experimental maximum adsorption capacity (Q_{max}) for ^{99}Mo(VI), 0.5 g of the adsorbent were contacted with 5 mL of the adsorbates solution for 2 h at 30 °C at initial concentration 144 mg L^{-1}. After equilibration, the solid phase was separated by centrifugation and the radioactivity of ^{99}Mo(VI) in the supernatant was assayed radiometrically by using a computerized multichannel analyzer of CANBERRA Genie 2000 type, model 5504c (USA) connected to a well-type NaI scintillation detector. The data obtained before and after the sorption process were used to calculate the uptake percentage (uptake %), distribution coefficient (K_d L g^{-1}) and adsorbed amount (q mg g^{-1}) according to the following equations:

$$\text{Uptake}\,\% = \frac{\text{Ao} - \text{A}}{\text{Ao}} \times 100 \quad (1)$$

$$\text{K}_\text{d} = \frac{\text{Ao} - \text{A}}{\text{A}} \times \frac{\text{V}}{\text{M}} \quad (2)$$

$$q = \frac{\text{Uptake}\,\% \times C_{\text{initial}} \times V}{100 \times M} \quad (3)$$

where A_o and A are the areas under the γ-ray peaks of the given radionuclide before and after adsorption onto the synthesized Co(II)–Fe(III) LDH respectively. V is the volume of the aqueous phase (mL) and M is the mass of Co(II)–Fe(III) LDH (g).

Desorption experiments

For desorption studies, 0.04 g Co(II)–Fe(III) LDH were contacted with 5 mL ^{99}Mo(VI) at pH ≈ 3.5 for 24 h. ^{99}Mo(VI) loaded on LDH sorbent was separated by centrifugation. The collected solid phases were contacted with 5 mL of the desorbing agents (NaCl, Na_2CO_3, Na_2SO_4 and $NaNO_3$) solutions at different concentrations (5×10^{-3}–1×10^{-2} M) and aged under shaking for 24 h. After centrifugation and measuring the radioactivity of ^{99}Mo(VI) radionuclides in the supernatant, the desorption percentage (desorption %) of the concerned radionuclide was calculated using the following equation:

$$\text{Desorption}\,\% = \frac{\text{Amount of adsorbate desorbed}}{\text{Amount of adsorbate adsorbed}} \times 100 \quad (4)$$

Results and discussion

Characterization of Co(II)–Fe(III) LDH

Surface area measurements

The surface properties of Co(II)–Fe(III) LDH are considered one of the main factors that could affect sorption process. The specific surface area and pore volume of synthesized material before and after sorption of Mo(VI) ions was measured using nitrogen gas adsorption and desorption isotherms. The synthesized Co(II)–Fe(III) LDH attained a high surface area of.

99 m^2g^{-1}. Also, the total pore volume was found to be 0.1 cm^3 g^{-1}, while pore radius is 7.2 A°. The high surface area and porosity could increase the sorption capacity of material towards molybdate anions. The textural properties of Co(II)–Fe(III) LDH are reduced after sorption of Mo(VI) anions. This is might be due to the adsorption of some of molybdate anions on the surface of Co(II)–Fe(III) LDH, while the others were diffused into pores.

FT-IR spectra

The FT-IR spectra of Co(II)–Fe(III) LDH before and after ^{99}Mo(VI) adsorption are shown in Fig. 1. It can be notice from this figure a broad strong absorption peak around 3390 Cm^{-1} is attributed to stretching vibrations of interlayer water molecules and hydroxyl group in LDH [35, 36]. Another smaller absorption peak appeared at around 1621 cm^{-1} is corresponding to bending mode of water molecules. The absorption bands at 656, 568 and 473 cm^{-1} are attributed to the Fe–O and Co–O lattice vibrations [37]. As can be notice from Fig. 1 the spectrum for Co(II)–Fe(III) LDH before adsorption of Mo is similar to that after adsorption. This means that there is no chemical reaction between the synthesized LDH and ^{99}Mo(VI).

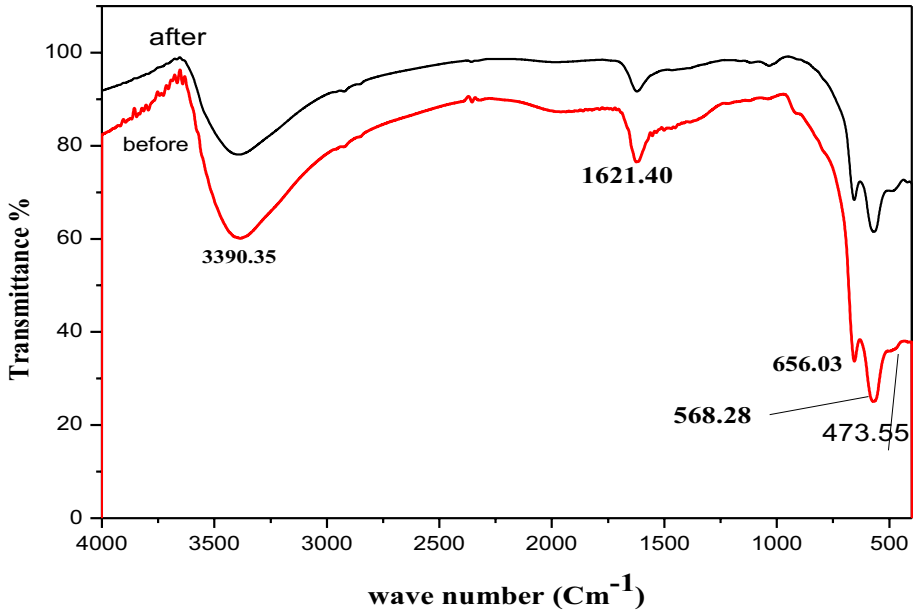

Fig. 1 FTIR spectrum of Synthesized Co(II)–Fe(III) LDH before and after adsorption of ^{99}Mo(VI)

XRD diffraction

Figure 2 represents XRD pattern of the synthesized material. This figure shows the appearance of diffraction peaks at 2Θ values of 11, 23, 31, 36, 60 and 64 which are characteristics for layer double hydroxide materials [30].

Effect of the solution pH

For studying an adsorption system, it is well- known that the pH of the solution is one of the most important parameters that should be investigated. This is because it not only affects the aqueous speciation of the adsorbate but also the surface chemistry of the adsorbent. Accordingly, the effect of the solution pH on the adsorption process of ^{99}Mo(VI) onto the synthesized Co(II)–Fe(III) LDH is studied in the pH range 3–13 at V/m ratio, equilibrium time and a temperature of 0.1 L g^{-1}, 2 h and 30 ± 1 °C, respectively. The obtained results (Fig. 3a) show that almost complete uptake percentage is achieved in the pH range of 3–11. Furthers increase in the pH giving rise to a sharp decrease in the uptake percentage that reached to about 15% at pH 13.

For interpretation of the data given in (Fig. 3a), the aqueous species of ^{99}Mo(VI) at the studied pH range is calculated using phreeqi software and the data are shown in (Fig. 3b). Based on these calculations, it is found that H_2MoO_4, $HMoO_4^-$ and MoO_4^{2-} are the dominant species of ^{99}Mo(VI) in the pH range 3–6. While, MoO_4^{2-} is the dominant one at pH values higher than 6. For the employed adsorbent $CoCl_2$ and $FeCl_3$ were used as precursors during synthesis of Co(II)–Fe(III) LDH. This implies that Cl^- ions are intercalated at the interlayer region. Therefore the removal achieved for ^{99}Mo(VI) anionic species ($HMoO_4^-$ and MoO_4^{2-}) could be attributed to the anion exchange of these species with Cl^- at the interlayer

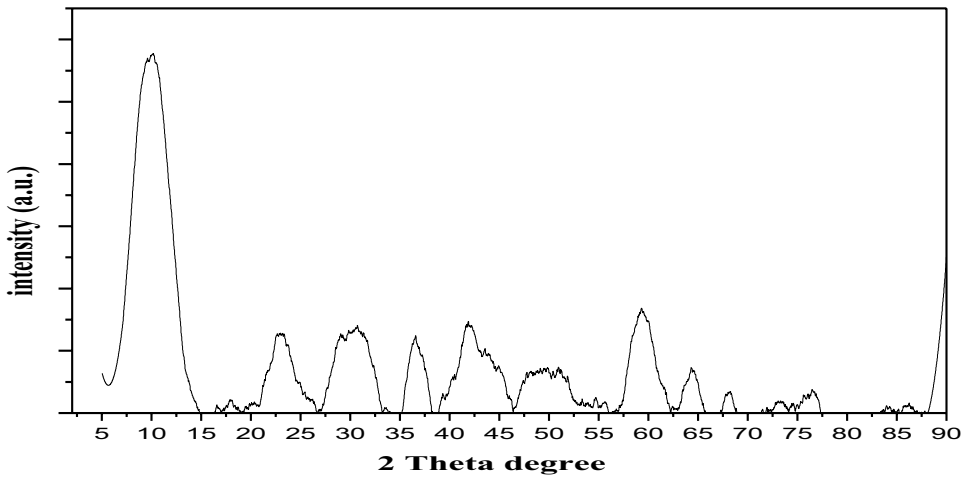

Fig. 2 XRD diffraction of Synthesized Co(II)–Fe(III) LDH

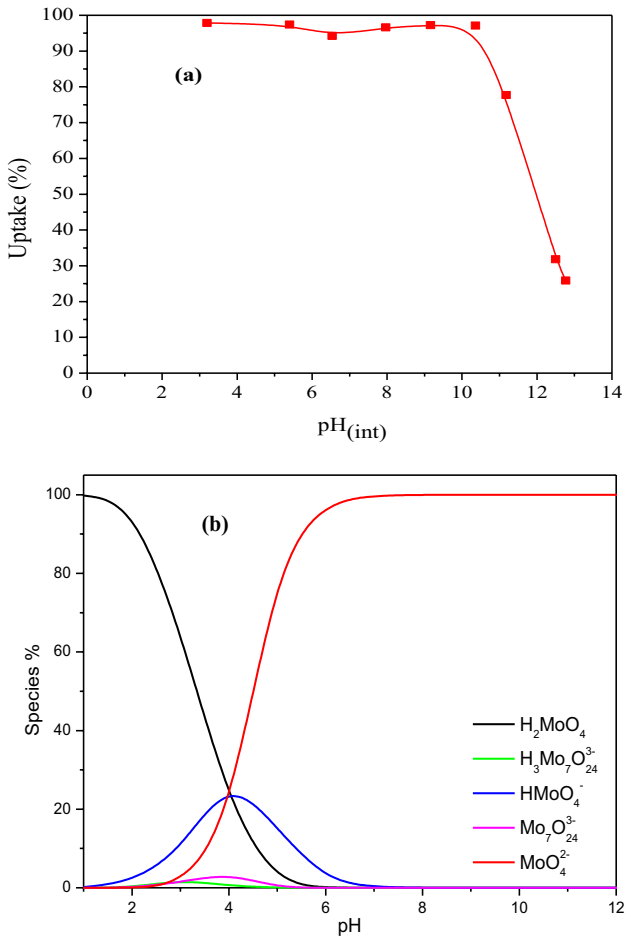

Fig. 3 Effect of pH on ^{99}Mo(VI) adsorption on LDH (**a**), and speciation of Mo(VI) at different pH values (**b**) (C_o = 50 mg L^{-1}, contact time = 2 h, Temp. = 30 ± 1 °C and V/m = 0.1 L g^{-1})

region. While the competition between OH^- and MoO_4^{2-} can be considered the main reason for the reduction in ^{99}Mo(VI) uptake at pH values higher than 11. At the lower studied pH values, particularly at pH 3, the data given in Fig. 11 confirm the efficiency of the synthesized LDH to uptake ^{99}Mo(VI) where uptake percentages > 99% are obtained although 60% of ^{99}Mo(VI) presents in the aqueous solution as H_2MoO_4. The uptake of this species is ascribed to the formation of hydrogen bonds with hydroxyl groups at the LDH surface. Based on these results and discussion, the adsorption mechanism of ^{99}Mo(VI) onto the synthesized Co(II)–Fe(III) LDH is suggested and represented in Fig. 4.

Effect of contact time

The impact of contact time, in the range of 1–1440 min, on the adsorption of ^{99}Mo(VI) onto LDH sorbent material is investigated at pH values of 3.5 and 9.3. The results obtained are represented in Fig. 5. The data given in this figure demonstrate that adsorption of ^{99}Mo(VI) onto the synthesized Co(II)–Fe(III) LDH was a rapid process particularly in the first five minutes where uptake percentage of 82% and 54% are achieved at pH values of 3.5 and 9.3, respectively. Thereafter, the uptake percentage is gradually increase with increasing contact time and the equilibrium is attained at 100 and 120 min with maximum uptake percentage values of about 80% and 98% at pH values of 9.3 and 3.5, respectively. The rapidity of ^{99}Mo(VI) adsorption in the first five minutes suggests the potential utilization the synthesized Co(II)–Fe(III) LDH as a good generator for ^{99m}Tc, which will be the future work in our laboratory. Based on the data depicted in Fig. 5, the adsorption experiments conducted in the present work were equilibrated for 120 min.

Modeling of kinetic data

Generally, it is known that estimating the kinetic parameters facilitates the design of an adsorption experiment. The kinetic data of ^{99}Mo(VI) onto LDH material Fig. 5 are analyzed by two commonly used adsorption kinetic models. These models are pseudo-first-order (Eq. 5) and the pseudo-second-order (Eq. 6) equations which are expressed as follow [38]

$$\ln(q_e - q_t) = \ln q_e - k_1 t \tag{5}$$

$$\frac{t}{q_t} = \frac{1}{k_s q_e^2} + \frac{1}{q_e} t \tag{6}$$

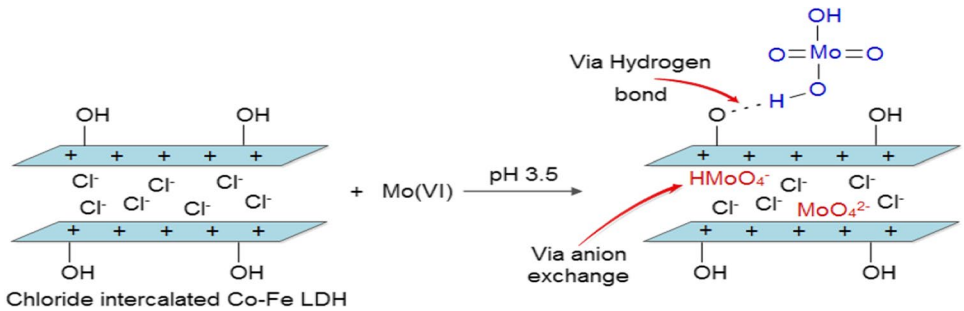

Fig. 4 Schematic representation of the proposed adsorption mechanism of ^{99}Mo(VI) onto the synthesized Co(II)–Fe(III) LDH

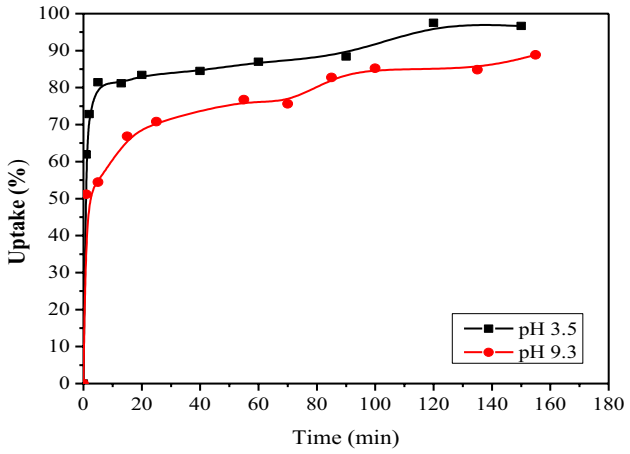

Fig. 5 Effect of contact time on the adsorption of ^{99}Mo(VI) on LDH at different pH (3.5 ± 0.05 and 9.3 ± 0.05) (C_o = 50 mg L^{-1}, Temp. = 30 ± 1 °C and V/m = 0.125 L g^{-1})

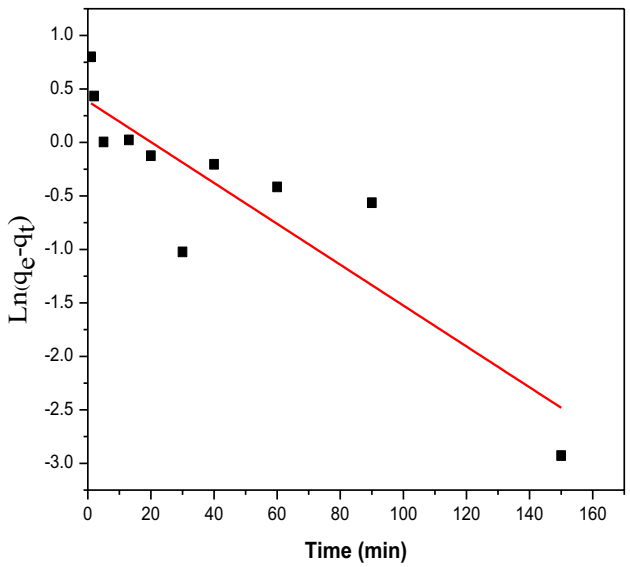

Fig. 6 Pseudo-first- order kinetic plots for the sorption of ^{99}Mo(VI) on LDH (Co = 50 mg L^{-1}, pH = 3.5 ± 0.05, and V/m = 0.125 L g^{-1})

where q_e and q_t are the amount of adsorbate uptake by the adsorbent at equilibrium (mg g^{-1}), at a given time (t) respectively, while K_1 and K_2 are the rate constants (min^{-1}).

Figures 6 and 7 depict linear fits of the experimental kinetic data of ^{99}Mo(VI) onto the LDH to the two previous kinetic models and Table 1 lists the calculated kinetic parameters and correlation coefficients (R^2).

According to the data given in this Table 1, it can be observed that the pseudo–second order kinetic model exhibited a higher correlation coefficient value (R^2 = 0.996) than the pseudo first order one (R^2 = 0.766). Herein, it is concluded that the present adsorption process of ^{99}Mo(VI) onto

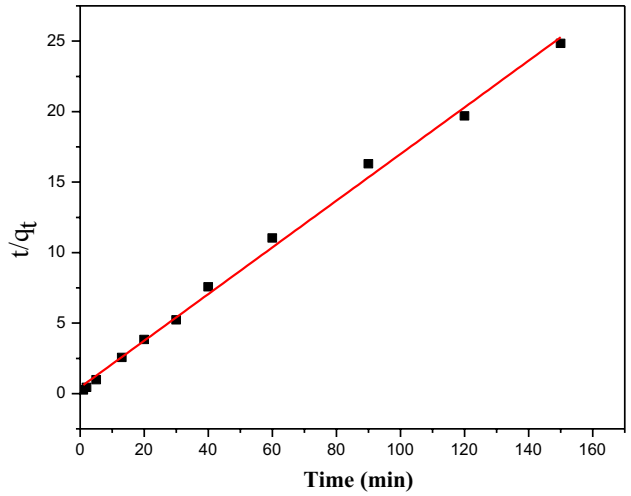

Fig. 7 Pseudo-second-order kinetic plots for the sorption of ^{99}Mo(VI) on LDH (Co = 50 mg L^{-1}, pH = 3.5 ± 0.05, and V/m = 0.125 L g^{-1})

Table 1 Adsorption kinetic parameters for adsorption of ^{99}Mo(VI) onto Co(II)–Fe(III) LDH

Kinetic model	Parameters	Value
Pseudo-first-order	K_1, min^{-1}	0.019
	q_e, mg g^{-1}	1.469
	R^2	0.766
Pseudo-second-order	K_2, g mg^{-1} min^{-1}	0.0624
	q_e, mg g^{-1}	6.041
	R^2	0.996

the synthesized LDH is well–fitted by the pseudo second order kinetic model.

Effect of adsorbent mass

Determining the lowest adsorbent mass necessary to achieve the best removal efficiency of an adsorbent toward an adsorbate material is often significant from the economic and waste management points of view. Therefore, the effect of the V/m ratio (0.05–1 L g^{-1}) on the adsorption of ^{99}Mo(VI) at pH = 3.5 onto Co(II)–Fe(III) LDH is studied and the results obtained are shown in Fig. 8. As can be observed from this figure, decreasing the LDH V/m from 1 to 0.05 L g^{-1} increased the uptake % from 45 to 98% whereas decreased the adsorbed amount from 23 to 2.5 mg g^{-1}. The increase of uptake percent with decreasing V/m values is attributed to the increase of the number of functional groups at the Co(II)–Fe(III) surface. The probability of collisions between LDH particles at higher adsorbent masses increased particles aggregation and the diffusion path length while the surface area of the solid phase decreased. Accordingly, the adsorption capacity of the synthesized LDH towards ^{99}Mo(VI) is

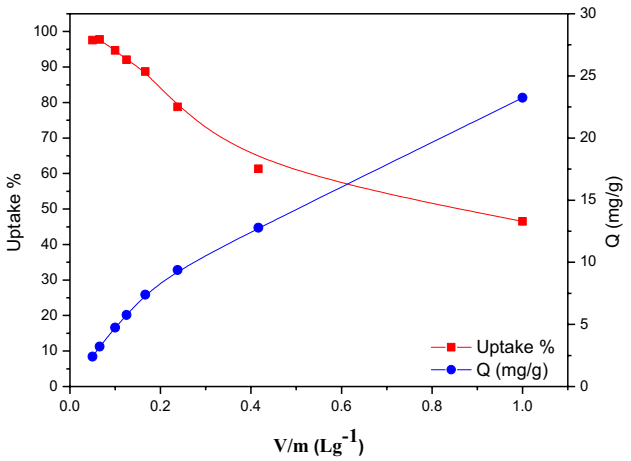

Fig. 8 Effect of V/m (L g^{-1}) on the adsorption of ^{99}Mo(VI) on LDH (C_o = 50 mg L^{-1}, contact time = 2 h Temp. = 30 ± 1 °C and pH = 3.5 ± 0.05)

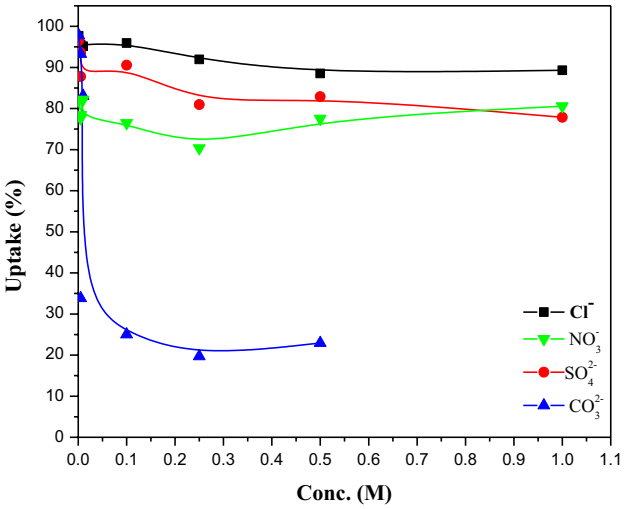

Fig. 9 Effect of foreign anions on adsorption of ^{99}Mo(VI) on LDH (C_o = 50 mg L^{-1}, pH = 3.5 ± 0.05, contact time = 2 h and V/m = 0.125 L g^{-1})

decreased with decreasing the V/m value. Based on the data given in Fig. 8, 0.125 L g^{-1} was chosen to be the optimum V/m value for conducting the adsorption experiments of this work.

Effect of foreign anions

One of the most important parameters that should be studied is the factor of foreign ions. Based on this parameter the ability of the adsorbent LDH material to remove ^{99}Mo(VI) from liquid waste containing coexisting anions could be estimated. Therefore, The impact of the foreign anions (Cl^-, NO_3^-, SO_4^{-2} and CO_3^{-2}) at different concentrations on adsorption of ^{99}Mo(VI) on LDH is investigated at C_o = 50 mg L^{-1}, pH = 3.5, contact time = 2 h and V/m = 0.125 L g^{-1}. The results obtained are shown in Fig. 9. This figure represents that Cl^- ion mostly had no effect on the adsorption efficiency of ^{99}Mo(VI) where recovery value more than 90% are achieved at the studied concentration range. For NO_3^- and SO_4^{2-} anions, it is found that the recovery value decrease from 99 to about 80% with increasing these concentration from 5×10^{-4} to 1 mol L^{-1}. on the other hand, adsorption of ^{99}Mo(VI) radionuclides when coexisted with CO_3^{2-} anions resulted into a sharp decrease in the recovery percentage. This sharp decrease can be attributed to the alteration of the solution pH to higher values. Accordingly, the aqueous species of Mo(VI) at pH 3.5(H_2MoO_4, $HMoO_4^-$, MoO_4^{2-}, $H_3MoO_{24}^{3-}$and $Mo_7O_{24}^{6-}$) are changed to MoO_4^{2-} which is the predominant species at pH values higher than 6. Herein the abrupt reduction in the recovery percentage of ^{99}Mo(IV) is ascribed to the competition between $^{99}MoO_4^{2-}$ and CO_3^{2-} for intercalation into Co(II)–Fe(III) layered double hydroxide. For the other studied anions, it is found that thesis coexistence with ^{99}Mo(VI) had no influence on the solution pH. Therefore, this deleterious effect is attributed to the competition between the predominant ^{99}Mo(VI) anionic species at pH 3.5 ($HMoO_4^-$ and MoO_4^{2-}) and the foreign anions (Cl^-, NO_3^- or SO_4^{2-}). Since these anion slightly decrease the recovery percentage of ^{99}Mo(VI) this completion with thesis completion with this anionic species only, it can be concluded that about 45% of ^{99}Mo(VI) that exist at pH 3.5 as H_2MoO_4 are adsorbed onto Co(II)–Fe(III) layered double hydroxide via formation of hydrogen bond rather than anionic exchange.

Thermodynamic studies

The influence of temperature on adsorption of ^{99}Mo(VI) on the synthesized LDH was investigated in the rang 20–50 °C, and the results are presented in Fig. 10. This figure shows that temperature played a significant role in the present adsorption process. By increasing temperature from 20 to 50 °C, the distribution coefficient value is increased from 0.75 to 3 L g^{-1}. this enhancement in the K_d value suggested that adsorption of ^{99}Mo(VI) onto Co(II)–Fe(III) LDH is endothermic process.

Based on the data given in Fig. 10, free energy change (ΔG°) of the present adsorption process is calculated using the following equation [39]

$$\Delta G^o = -RTlnK_d \quad (7)$$

where R is the universal gas constant (R = 0.008314 kJ/mol) and T is the absolute temperature in Kelvin. While the other thermodynamic parameters enthalpy change (ΔH)

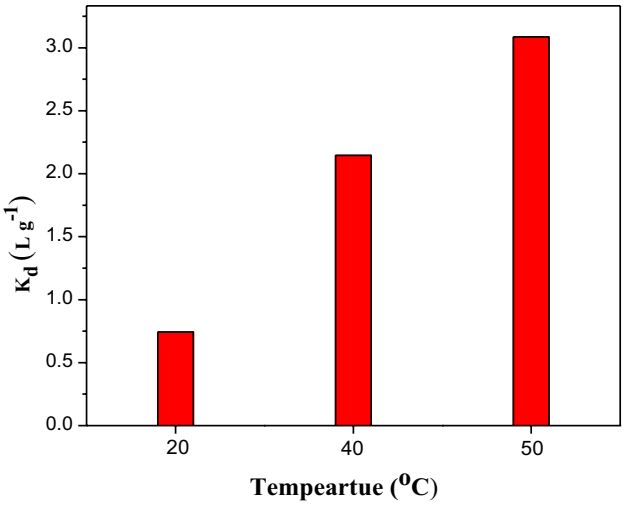

Fig. 10 Effect of temperature on sorption of ^{99}Mo(VI) on LDH (C_o = 200 mg L^{-1}, pH = 3.5 ± 0.05, Contact time = 2 h and V/m = 0.1 L g^{-1})

and entropy change (ΔS°) are calculated according to the following relation [39]:

$$\ln K_d = \frac{\Delta S^o}{R} - \frac{\Delta H^o}{RT} \quad (8)$$

Values of ΔS° and ΔH° are estimated by from intercept and slope of the linear plot of Ln K_d versus $\frac{1}{T}$, respectively. The obtained values are recorded in Table 2. This table shows that the free energy change exhibited a positive value (ΔG° = 0.691 kJ/mol) at 20 °C while negative values (ΔG° = − 1.847 and − 3.160 kJ/mol) at higher temperatures. These data indicate that adsorption of ^{99}Mo(VI) onto Co(II)–Fe(III) LDH was more spontaneous and thus more favorable at higher temperatures. Besides, the ΔG values especially at the higher studied temperatures suggested that physical adsorption was the main mechanism for recovery of ^{99}Mo(VI) by the concerned adsorbent. On the other hand, the positive value of enthalpy change (ΔG° = 37.873 kJ/mol) confirmed that the present adsorption process was endothermic in nature. Eventually, the positive entropy change (ΔS° = 0.127 kJ/mol K) indicated the increase of randomness at the solid- liquid interface.

Table 2 Thermodynamic parameters for adsorption of ^{99}Mo(VI) onto Co(II)–Fe(III) LDH

Temperature (K)	$\Delta G°$ (kJ mol^{-1})	$\Delta H°$ (kJ mol^{-1})	$\Delta S°$ (kJ mol^{-1} K^{-1})
293	0.691	37.873	0.127
313	− 1.847		
323	− 3.160		

Adsorption isotherm

The effect of the initial ion concentration of ^{99}Mo(VI) in the range 4.5–350 mg L^{-1} on its adsorption on Co(II)–Fe(III) LDH is studied at pH = 3.1. As can be seen by the data depicted in Fig. 11, the uptake percentage of ^{99}Mo(VI) is significantly influenced by its initial concentration in the working solution. By increasing the initial concentration from 10 to 350 mg L^{-1}, the uptake percentage is decreased from 99.8 to 63%, which can be ascribed to saturation of Co(II)–Fe(III) LDH sites. On the contrary, the experimental data given in Fig. 11 show that the adsorbed amount of ^{99}Mo(VI) is greatly improved with increasing is initial concentration. This enhancement is attributed to the increase of the mass driving force of ^{99}Mo(IV) towards the synthesized LDH.

In current study, three non-linear isotherm models are applied to analyze the adsorption isotherms of ^{99}Mo(VI) onto Co(II)–Fe(III) LDH material. These models are Freundlich (Eq. 9), Langmuir (Eq. 10) and Temkin (Eq. 11) which are represented by the following equations [40]

$$q_e = K_F C_e^{1/n} \quad (9)$$

$$q_e = \frac{q_m K_L C_e}{1 + K_L C_e} \quad (10)$$

$$q_e = B_T Ln A_T C_e \quad (11)$$

where C_e is the ^{99}Mo(VI) equilibrium concentration (mg L^{-1}), q_e is the amount of adsorbate uptaken (mg g^{-1}) and q_m is the maximum adsorption capacity (mg g^{-1}).

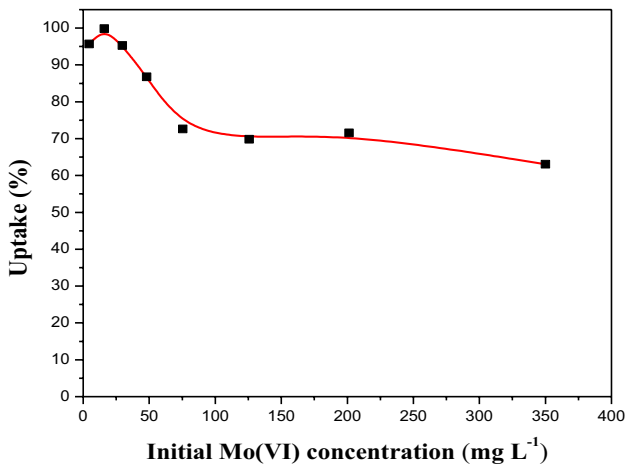

Fig. 11 Effect of initial concentration on sorption of ^{99}Mo(VI) on LDH (pH = 3.1 ± 0.05, contact time = 2 h and V/m = 0.125 L g^{-1})

Non Linear fitting of the experimental adsorption isotherm data of ^{99}Mo(VI) onto Co(II)–Fe(III) LDH, by the non- linear method of analysis using Origin Pro 8.5 software, to the aforementioned isotherm models (Eqs. 8–10) are represented in Fig. 12 values of the obtained isotherm parameters, correlation coefficient R^2 and error functions, reduced chi- square (χ^2) and residual sum of square (RSS), are recorded in Table 3. The significant low in the correlation coefficient value resulted from evaluating Temkin isotherm model ($R^2 = 0.667$) for the present adsorption isotherm data suggested it's in applicability. On the other hand, Freundlichs isotherm model shows a higher correlation value ($R^2 = 0.991$) than Langmuir ($R^2 = 0.969$), with lower values for reduced chi-square (χ^2 equals 0.796 for Freundlichs and 3.047 for Langmuir) and residual sum of square (RSS equals 3.978 and 15.233 for Freundlichs and Langmuir, respectively).Based on these findings, it is concluded that Freundlichs is the best isotherm models for describing the present experimental adsorption data of ^{99}Mo(VI) onto the synthesized Co(II)–Fe(III) LDH.

Maximum adsorption capacity and comparison with other studies

The data given in the present research work indicate that ^{99}Mo(VI) was efficiently recovered by Co(II)–Fe(III) through a wide pH range of 3–10.5. To further evaluated the efficiency of the synthesized LDH, its maximum adsorption capacity towards ^{99}Mo(VI) radionuclides was experimentally determined at pH 3.5. It is found that Co(II)–Fe(III) LDH had a maximum adsorption capacity of 255.175 mg g^{-1} for ^{99}Mo(VI). By comparing this value with those reported in literature using other adsorbents Table 4, it is concluded that the synthesized Co(II)–Fe(III) show a comparable value.

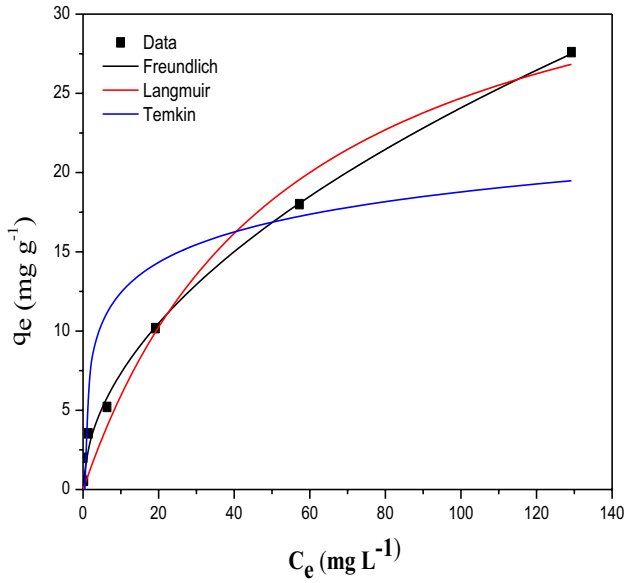

Fig. 12 Non–linear models Freundlich, Langmuir and Temkin

Table 3 Isotherm parameters for adsorption of ^{99}Mo(VI) onto Co(II)–Fe(III) LDH

Isotherm model	Parameters and error functions	Value
Langmuir	q_m Model (mg g^{-1})	38.117
	K_L (L mg^{-1})	0.018
	R_L	0.425
	R^2	0.969
	χ^2	3.047
	RSS	15.233
Freundlich	K_F (mg $^{1-(1/n)}$ $L^{1/n}$ g^{-1})	2.236
	1/n	0.516
	R^2	0.991
	χ^2	0.796
	RSS	3.978
Temkin	K_T (L g^{-1})	9.037
	b (kJ mol^{-1})	2.758
	R^2	0.667
	χ^2	32.751
	RSS	163.754

Desorption study

Desorption of ^{99}Mo(IV) loaded onto Co(II)–Fe(III) LDH is investigated using various desorbing agents (NaCl, $NaNO_3$, Na_2SO_4 and Na_2CO_3) at the concentration range of 5×10^{-4}–1×10^{-2} mol L^{-1}. The results obtained are represented in Fig. 13. This figure demonstrates that Cl^-, $NO_3^-$and SO_4^{2-} mostly failed to desorb ^{99}Mo(VI) ions even at high concentrations where maximum desorption percentage of about 10% is recorded using 1×10^{-2} mol L^{-1} SO_4^{2-}.whereas, 42% of ^{99}Mo(VI) loaded onto Co(II)–Fe(III) LDH is desorbed using CO_3^{2-} at the higher studied concentration, which is attributed to replacement of ^{99}Mo(VI) anionic species ($HMoO_4^-$ and MoO_4^{2-}) with CO_3^{2-} ones. The inability of CO_3^{2-} to completely desorb ^{99}Mo(VI) loaded to LDH is presumably attributed to adsorption of large amount of ^{99}Mo(VI) as H_2MoO_4 species via formation of hydrogen bond with the adsorbent.

Conclusions

Co(II)–Fe(III) LDH material was successfully synthesized and employment as an adsorbent for uptake of ^{99}Mo(VI) from aqueous solutions. The data showed that the synthesized LDH had the efficiency to uptake ^{99}Mo(VI), uptake % ≈ 98, through a wide pH range of 3–10. This implies that Co(II)–Fe(III) LDH succeeded to adsorb the different

Table 4 Comparison of the maximum sorption capacity of LDH for ^{99}Mo(VI) with other sorbents

Sorbent	Q_{max} (mg g^{-1})	References
Metal–organic framework UiO-66	335	[41]
Mesoporous aluminum oxides (mesoporous aluminum oxides)	112	[6]
Insoluble chitosan sorbent	123	[42]
Mg–Fe–NO_3–LDH	21.3	[43]
Iron-based adsorbents	8.3126	[44]
Strong (Amberlite IRA-400)	177	
Weak (Amberlite IRA-743)	208	[45]
Mesoporous aluminum oxides	112	[6]
Starch-acrylamide/nanohalloysite composite	524	[46]
$ZnCl_2$ activated carbon developed from coir pith	18.9	[47]
Co(II)–Fe(III) LDH	255.175	This work

predominant species of ^{99}Mo(VI) present in aqueous solution which includeH_2MoO_4, $HMoO_4^-$ and MoO_4^{2-} in this pH range. The kinetic data at pH 3.5 showed that 2 h were sufficient to attain equilibrium and these data were better fitted by the pseudo-second order kinetic model than the pseudo – first- order one. Of the studied isotherm models, Freundlich was the best one for fitting the adsorption equilibrium data. Experimental determining of the adsorption capacity of Co(II)–Fe(III) LDH toward ^{99}Mo(VI) at pH 3.5 resulted into a maximum value of about 255 mg g^{-1}. The calculated values of the free energy change revealed that adsorption of ^{99}Mo(VI) onto LDH was more spontaneous at the higher studied temperature and the enthalpy change value ($\Delta H^{\circ} = 37.873$ kJ/mole) indicated that it was an endothermic process. Although various desorbing agents at different concentrations were evaluated for desorption of ^{99}Mo(VI) loaded onto Co(II)–Fe(III) LDH, but maximum desorption percentage of about 40% was achieved by 1×10^{-2} mol L^{-1} Na_2CO_3. Adsorption of ^{99}Mo(VI) onto the synthesized LDH at pH 3.5 was suggested to proceed via formation of hydrogen bond (through H_2MoO_4 species) and anion exchange between its anionic species ($HMoO_4^-$ and MoO_4^{2-}) and Cl^- anions at the inter layer region of Co(II)–Fe(III) LDH.

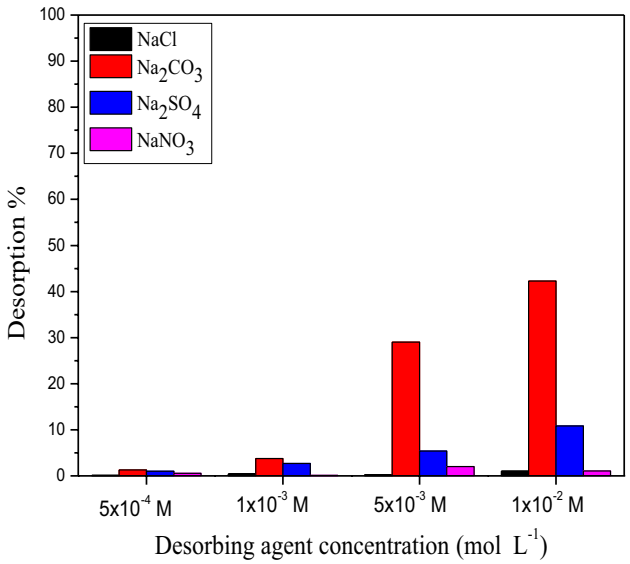

Fig. 13 Desorption of ^{99}Mo(VI) by different concentration solutions

Author contributions All authors contributed to the study conception and design. Material preparation, data collection and analysis were performed by MAG, MAH and MAA. The first draft of the manuscript was written by MAG and reviewed by MRM and all authors commented on previous versions of the manuscript. All authors read and approved the final manuscript.

Funding Open access funding provided by The Science, Technology & Innovation Funding Authority (STDF) in cooperation with The Egyptian Knowledge Bank (EKB). The authors declare that no funds, grants, or other support were received during the preparation of this manuscript.

Data availability All data and materials included in the submitted manuscript will be available upon request.

Declarations

Conflict of interest The authors declare that they have no conflict of interests.

References

1. Filzen LM, Ellingson LR, Paulsen AM, Hung JC (2017) Potential ways to address shortage situations of ^{99}Mo/^{99m}Tc. J Nucl Med Technol 45:1. https://doi.org/10.2967/jnmt.116.185454
2. Firestone RB, Corralled M, Frank SY (1998) Table of isotopes, 8th edn. Wiley, New York
3. Marlina E, Lestari A, Hambali I, Saptiama S, Febriana K, Awaludin R, Tanase M, Nishikata K, Tsuchiya K (2010) Molybdenum-99 (^{99}Mo) adsorption profile of zirconia-based materials for ^{99}Mo/^{99m}Tc generator application. Atom Indonesia 46(2):91–97. https://doi.org/10.17146/aij.2020.914
4. Liem PH, Tran HN, Sembiring TM (2015) Design optimization of a new homogeneous reactor for medical radioisotope Mo-99/Tc-99m production. Prog Nucl Energy 82:191. https://doi.org/10.1016/j.pnucene.2014.07.040
5. Eckelman WC (2009) Unparalleled contribution of technetium-99m to medicine over 5 decades. J Am Coll Cardiol 2:364–368. https://doi.org/10.1016/j.jcmg.2008.12.013
6. Denkova AG, Denkova BE, Terpstra OM, Steinbach J, ten Dam H, Wolterbeek Th (2013) Adsorption of molybdenum on mesoporous aluminum oxides for potential application in nuclear medicine. Sep Sci Technol 48:1331–1338. https://doi.org/10.1080/01496395.2012.736443
7. El-Sweify FH, Abdel Fattah AA, El-Sheikh R, Aly SM, Ghamry MA (2017) Studies on ^{99}Mo–^{99m}Tc adsorption and elution behaviors using the inorganic sorbent ceric tungstate and conventional organic resins. Radiochim Acta 105(7):561–568. https://doi.org/10.1515/ract-2016-2665
8. Hamed MM, Rizk HE, Ahmed IM (2018) Adsorption behavior of zirconium and molybdenum from nitric acid medium using low-cost adsorbent. J Mol Liq 249:361–370. https://doi.org/10.1016/j.molliq.2017.11.049
9. Nguyen M, Hong T, Man SL (2013) Separation of molybdenum and vanadium from acid solutions by ion exchange. Hydrometallurgy 136:65–70. https://doi.org/10.1016/j.hydromet.2013.03.007
10. Zeng L, Chu YC (2010) Recovery of molybdenum and vanadium from synthetic sulphuric acid leach solutions of spent hydrodesulphurisation catalysts using solvent extraction. Hydrometallurgy 101:141–147. https://doi.org/10.1016/j.hydromet.2009.12.008
11. Li J, Zhao Z, Cao C, Zhang G, Huo G (2012) Recovery of Mo from Ni–Mo ore leach solution with carrier co-precipitation method. Int J Refract Hard Met 30:180–184. https://doi.org/10.1016/j.ijrmhm.2011.08.005
12. Verbinnen B, Block C, Hannes D, Lievens P, Vaclavikova M, Stefusova K, Vandecasteele C (2012) Removal of molybdate anions from water by adsorption on zeolite-supported magnetite. Water Environ Res 84(9):753–760. https://doi.org/10.2175/106143012X13373550427318
13. Fourie M, Meyer WC, van der Westhuizen DJ, Krieg HM (2016) Uranium recovery from simulated molybdenum-99 production residue using non-dispersive membrane based solvent extraction. Hydrometallurgy 164:330–333. https://doi.org/10.1016/j.hydromet.2016.07.001
14. Park K, Hong IK, Parhi PK (2010) Recovery of molybdenum from spent catalyst leach solutions by solvent extraction with LIX 84-I. Sep Purif Technol 74(3):294–299. https://doi.org/10.1016/j.seppur.2010.06.018
15. Rout PC, Sarangi K (2013) A comparative study on extraction of Mo (VI) using both solvent extraction and hollow fiber membrane technique. Hydrometallurgy 133:149–155. https://doi.org/10.1016/j.hydromet.2013.01.005
16. Chakravarty R, Ram R, Dash A, Pillai MRA (2012) Preparation of clinical-scale ^{99}Mo/^{99m}Tc column generator using neutron activated low specific activity ^{99}Mo and nanocrystalline γ-Al_2O_3 as column matrix. Nucl Med Biol 39(7):916–922. https://doi.org/10.1016/j.nucmedbio.2012.03.010
17. Awaludin R, Gunawan AH, Lubis H, Herlina S, Kimura A, Tsuchiya K, Tanase M, Ishihara M (2015) Mechanism of ^{99}Mo adsorption and ^{99m}Tc elution from zirconium based material in ^{99}Mo/^{99m}Tc generator column using neutron irradiated natural molybdenum. J Radioanal Nucl Chem 303:1481. https://doi.org/10.1007/s10967-014-3606-z
18. Tachibana Y, Yamazaki Y, Nomura M, Suzuki T (2015) Molybdenum isotope fractionation in ion exchange reaction by using anion exchange chromatography. J Radioanal Nucl Chem 303:1429. https://doi.org/10.1007/s10967-014-3510-6
19. Mertinez-Baez E, Dominguez J, Sahyli Ortega-Pijeira M, Tejeda- Mazola Y, Borroto J, Rivera-Denis A (2016) Synthesis and evaluation of ferragels as prospective solid ^{99m}Tc radiotracers. J Radioanal Nucl Chem 304:267. https://doi.org/10.1007/s10967-014-3766-x
20. Saptiama I, Kaneti YV, Suzuki Y, Tsuchiya K, Fukumitsu N, Sakae T, Yamauchi Y (2018) Template-free fabrication of mesoporous alumina nanospheres using post-synthesis water-ethanol treatment of monodispersed aluminium glycerate nanospheres for molybdenum adsorption. Small 14(21):1800474. https://doi.org/10.1002/smll.201800474
21. Wang Y, Qi Y, Li Y, Wu J, Ma X, Yu C, Ji L (2013) Preparation and characterization of a novel nano-absorbent based on multi-cyanoguanidine modified magnetic chitosan and its highly effective recovery for Hg(II) in aqueous phase. J Hazard Mater 260:9–15. https://doi.org/10.1016/j.jhazmat.2013.05.001
22. Browne MP, Sofer Z, Pumera M (2019) Layered and two dimensional metal oxides for electrochemical energy conversion. Energy Environ Sci 12:41–58. https://doi.org/10.1039/C8EE02495B
23. Qin M, Liang H, Zhao X, Wu H (2020) Glycine-assisted solution combustion synthesis of $NiCo_2O_4$ electromagnetic wave absorber with wide absorption bandwidth. Ceram Int. https://doi.org/10.1016/j.ceramint.2020.05.311
24. Deng X, Kang X, Xiang MLK, Wang C, Guo Z, Zhang J, Fu XZ, Luo JL (2020) Coupling efficient biomass upgrading with H_2 production via bifunctional CuxS@NiCo-LDH core–shell nanoarray electrocatalysts. J Mater Chem A 8:1138–1146. https://doi.org/10.1039/C9TA06917H
25. Nalawda P, Aware B, Kadam VJ, Hirlekar RS (2009) Layered double hydroxides: a review. J Sci Ind Res 68:267–272
26. Ye K, Lina Z, Shuai Z, Fazhi Z, Mingdong D, Sailong X (2010) Morphologies, preparations and applications of layered double hydroxide micro-/nanostructures. Materials 3:5220–5235. https://doi.org/10.3390/ma3125220
27. Cao Z, Li B, Sun L, Li L, Xu ZP, Gu Z (2020) 2D layered double hydroxide nanoparticles: recent progress toward preclinical/clinical nanomedicine. Small Methods 4:1900343. https://doi.org/10.1002/smtd.201900343
28. Jaehyuk K, Tatiana G, Sangsu P, Jueun K, Tamas V, Wooyong U (2020) Nanostructured Mg Fe and CoCr layered double hydroxides for removal and sequestration of iodine anions. J Chem Eng 380:122408. https://doi.org/10.1016/j.cej.2019.122408
29. Yanwei G, Zhiliang Z, Yanling Q, Jianfu Z (2012) Adsorption of arsenate on Cu/Mg/Fe/La layered double hydroxide from aqueous solutions. J Hazard Mater 239:279–288. https://doi.org/10.1016/j.jhazmat.2012.08.075
30. Mahamudur I, Rajkishore P (2010) Synthesis and physicochemical characterization of Zn/Al chloride layered double hydroxide and evaluation of its nitrate removal efficiency. Desalination 256:120–128. https://doi.org/10.1016/j.desal.2010.02.003
31. Susanta P, Jim HM, Joseph E (2013) Controls on arsenate, molybdate, and selenate uptake by hydrotalcite-like layered double

hydroxides. Chem Geol 345:130–138. https://doi.org/10.1016/j.chemgeo.2013.02.015
32. Nejati K, Akbari AR, Davari S, Asadpour-Zeynali K, Rezvani Z (2018) Zn–Fe-layered double hydroxide intercalated with vanadate and molybdate anions for electrocatalytic water oxidation. New J Chem 42(4):2889–2895. https://doi.org/10.1039/c7nj04469k
33. Ardau C, Frau F, Dore E, Lattanzi P (2012) Molybdate sorption by Zn–Al sulphate layered double hydroxides. Appl Clay Sci 65:128–133. https://doi.org/10.1016/j.clay.2012.05.005
34. Carla A, Franco F, Pierfranco L (2016) Antimony removal from aqueous solutions by the use of Zn–Al sulphate layered double hydroxide. Water Air Soil Pollut 227:344. https://doi.org/10.1007/s11270-016-3048
35. Nejati K, Rezvani Z, Mansorfar M, Anorg Z (2011) Adsorption of metanil yellow azoic dye from aqueous solution onto Mg–Fe–NO_3 layered double hydroxide Z. Anorg Allg Chem 637:1573–1579. https://doi.org/10.1002/zaac.201100132
36. Colthup NP, Daly LH, Stephen EW (1965) Introduction to infrared and Raman spectroscopy. Academic Press, London
37. Kamellia N, Ali RA, Soheila D, Karim A, Zolfaghar R (2018) Zn–Fe-layered double hydroxide intercalated with vanadate and molybdate anions for electrocatalytic water oxidation. New J Chem. https://doi.org/10.1039/c7nj04469k
38. El-Sweify FH, Abdel Fattah AA, Ghamry MA, Aly SM, El-Shahat MF (2020) Adsorption of ^{141}Ce(III), ^{160}Tb(III) and ^{169}Yb(III) on the synthesized inorganic ion exchanger, zirconium titanium phosphate. Radiochemistry 62(3):335–346. https://doi.org/10.1134/S1066362220030066
39. Hamoud MA, Allan KF, Ayoub RR, Holeil M, Mahmoud MR (2021) Efficient removal of radiocobalt and manganese from their binary aqueous solutions by batch adsorption Process using PAN/HDTMA/KCuHCF composite. Radiochim Acta 109:27–39. https://doi.org/10.1515/ract-2020-0078
40. Mahmoud MR, Rashad GM, Elewa AM, Metwally E, Saad EA (2019) Optimization of adsorption parameters for removal of $^{152+154}$Eu(III) from aqueous solutions by using Zn–Cu–Ni ternary mixed oxide. J Mol Liq 291:111257. https://doi.org/10.1016/j.molliq.2019.111257
41. Chao M, Alexandros V, Hubert T, Wolterbeek AGD, Pablo SC (2022) Adsorption of molybdenum on Zr-based MOFs for potential application in the ^{99}Mo/^{99m}Tc generator. Appl Surf Sci 572:151340. https://doi.org/10.1016/j.apsusc.2021.151340
42. Roxanne B, Jonathan G, Somayyeh N, Jean-Sébastien D, Bruno C (2018) Adsorption and desorption of molybdenum(VI) in contaminated water using a chitosan sorbent. J water process Eng 23:13–19. https://doi.org/10.1016/j.jwpe.2018.02.016
43. Li L, Qinghai G, Yaowu C (2019) Uptake of aqueous tungsten and molybdenum by a nitrate intercalated, pyroaurite-like anion exchangeable clay. Appl Clay Sci 180:105179. https://doi.org/10.1016/j.clay.2019.105179
44. Gjergj D, Toyohisa FTK, Jayappa M, Seiji M, Hideyuki T, Kazuyuki T (2011) Synthesis of iron-based adsorbents and their application in the adsorption of molybdenum ions in nitric acid solution. Chem Eng J 166:496–503. https://doi.org/10.1016/j.cej.2010.10.079
45. Izabela P, Piotr C, Bruno FU, Bernabé LR, Marek B, Nalan K (2017) Amberlite IRA-400 and IRA-743 chelating resins for the sorption and recovery of molybdenum(VI) and vanadium(V): equilibrium and kinetic studies. Hydrometallurgy 169:496–507. https://doi.org/10.1016/j.hydromet.2017.02.017
46. Elsharma EM, Emara AM, Abdelmonem IM, Gizawy MA (2022) High efficient removal of molybdenum (VI) from aqueous solution by starch-acrylamide/nanohalloysite composite Radiat. Phys Chem 201:110456. https://doi.org/10.1016/j.radphyschem.2022.110456
47. Namasivayam C, Sangeetha D (2006) Removal of molybdate from water by adsorption onto $ZnCl_2$ activated coir pith carbon. Bioresour Technol 97:1194–1200. https://doi.org/10.1016/j.biortech.2005.05.008